Integral Equation Solutions to Approximate the Average Run Length of a Long-Memory Seasonal Autoregressive Fractionally Integrated Moving Average Process on an EWMA Control Chart

Wilasinee Peerajit
Department of Applied Statistics, Faculty of Applied Science, King Mongkut's University of Technology North Bangkok, Thailand
wilasinee.p@sci.kmutnb.ac.th (corresponding author)

Yupaporn Areepong
Department of Applied Statistics, Faculty of Applied Science, King Mongkut's University of Technology North Bangkok, Thailand
yupaporn.a@sci.kmutnb.ac.th

Received: 8 March 2026 | Revised: 18 April 2026 | Accepted: 30 April 2026

 DOI: https://doi.org/10.48084/etasr.18603

ABSTRACT

This study evaluates the performance of the Exponentially Weighted Moving Average (EWMA) control chart for monitoring long-memory seasonal processes using a Numerical Integral Equation (NIE) approach, specifically a Seasonal Autoregressive Fractionally Integrated Moving Average (SARFIMA) process with exponential white noise. The metrics used include the Average Run Length (ARL), Standard Deviation of the Run Length (SDRL), and selected percentiles, which are derived using integral-equation formulations. The NIE method is applied using midpoint, trapezoidal, Simpson's, and Gauss–Legendre quadrature rules, after which monitoring is calibrated to achieve an in-control ARL of approximately 370 for smoothing parameter values of 0.05, 0.10, and 0.15. All quadrature schemes yield identical ARL results, differing only in computational efficiency. As the process mean shift magnitude is increased, the ARL, SDRL, and quartile measures decrease, thereby indicating faster and more stable detection. The practicability of the method is illustrated using monthly XAU/USD gold price data (January 2020 to February 2026), where the fitted SARFIMA model adequately captures seasonal long-memory dynamics and supports reliable EWMA monitoring performance.

Keywords-Numerical Integral Equation (NIE) method; Average Run Length (ARL); Standard Deviation of the Run Length (SDRL); Median Run Length (MRL); exponential white noise SARFIMA(1,d,1)(1,0,1)^{12} model

I. INTRODUCTION

Control charts are fundamental tools for monitoring production and service processes and are generally classified into memory-less and memory-type schemes. The Shewhart control chart, a classical memory-less approach, uses only the current observation and is mainly effective for detecting large shifts [1]. In contrast, memory-type control charts incorporate past information, with the Exponentially Weighted Moving Average (EWMA) [2] and Cumulative Sum (CUSUM) [3] charts being widely used for their superior sensitivity to small-to-moderate shifts. The EWMA control chart is attractive due to its simple structure, ease of implementation, and ability to smooth random variation while remaining sensitive to gradual or persistent shifts. By assigning exponentially decreasing weights to past observations, it balances recent and historical information, making it suitable for detecting subtle changes in time-dependent processes. Owing to these properties, EWMA has been widely applied in manufacturing, healthcare, financial, and environmental monitoring [4-6].

In practice, process observations often exhibit autocorrelation, which violates the independence and normality assumptions in classical control chart theory. Such dependence can be modeled using time-series approaches. The Autoregressive Fractionally Integrated Moving Average (ARFIMA) model extends the Autoregressive Integrated Moving Average (ARIMA) framework by introducing a

fractional differencing parameter to capture long-memory behavior [7-9], and its combination with the EWMA control chart has been extensively investigated (e.g., [10]). Adding a seasonal element results in the SARFIMA$(p,d,q)\times(P,D,Q)^S$ model; accommodating both long-range dependence and seasonal variation makes it particularly suitable for application to economic, environmental, and engineering data [11, 12].

The error term (white noise) in time-series models is often assumed to be Gaussian, albeit that this assumption is not always appropriate. White noise can be exponentially distributed, which has been shown to better represent certain real-world phenomena such as hydrological and environmental processes [13-15]. Consequently, monitoring procedures should account for both autocorrelation and non-normality simultaneously.

The performance of a control chart is typically evaluated through the run length of the accompanying process, defined as the number of plotted statistical points until the first out-of-control signal occurs. The most widely used measure is the Average Run Length (ARL), where a desirable scenario for a control chart comprises a large in-control ARL (ARL_0) to reduce false alarms and a small out-of-control ARL (ARL_1) to ensure rapid detection [1]. Additional measures, including Standard Deviation of the Run Length (SDRL) and the Run-Length Quartiles (RLQs), provide further insight into the variability and distributional behavior of control chart performance.

The ARL can be computed using Monte Carlo simulation, a Markov chain [16], or integral-equation techniques [17]. In particular, the Numerical Integral Equation (NIE) approach exploits the integral-equation representation of the RL distribution, thereby enabling analytical evaluation of ARL, SDRL, and RLQs [18, 19]. This approach approximates the ARL rather than providing an exact derivation. Because a comparable analytical formulation is not readily available for the CUSUM control chart in this setting, this approach is only considered for the EWMA control chart in the present study. The EWMA statistic allows an integral-equation representation of the run-length distribution, thereby enabling analytical evaluation of the performance measures (ARL, SDRL, and RLQs) for the control chart under the assumed model.

In the present study, the ARL is integrally approximated using the NIE method with various rules (Gauss–Legendre quadrature, midpoint, trapezoidal, and Simpson's) and extended to compute the SDRL and RLQs for a long-memory SARFIMA$(1,d,1)\times(1,0,1)^{12}$ process with exponential white noise.

II. EWMA CONTROL CHART FOR LONG-MEMORY SARFIMA PROCESSES WITH EXPONENTIAL WHITE NOISE

This section describes the structure of the EWMA control chart applied to a long-memory SARFIMA$(1,d,1)\times(1,0,1)^{12}$ process with exponential white noise. The methodology comprises process modeling and control chart construction.

The SARFIMA$(p,d,q)\times(P,D,Q)^S$ model can be defined as:

$$\phi_p(B)\Phi_P(B^S)(1-B)^d(1-B^S)^D X_t = \theta_q(B)\Theta_Q(B^S)\varepsilon_t \quad (1)$$

where B and B^S denote the non-seasonal and seasonal backward operators, respectively; X_t is the time series; ε_t denotes the exponential white noise. The backward-shift operator is defined as $BX_t = X_{t-1}$. In the above equation, polynomials $\phi_p(B)$ and $\Phi_P(B^S)$ correspond to the non-seasonal and seasonal autoregressive (AR) components of orders p and P, respectively, i.e.,

$$\begin{aligned}\phi_1(B)\Phi_1(B^{12}) &= (1-\phi_1 B)(1-\Phi_1 B^{12}) \\ &= 1-\phi_1 B-\Phi_1 B^{12}+\phi_1\Phi_1 B^{13}\end{aligned}$$

where $p = P = 1$, whereas $\theta_q(B)$ and $\Theta_Q(B^S)$ denote the non-seasonal and seasonal moving average (MA) components of orders q and Q, respectively, i.e.,

$$\begin{aligned}\theta_1(B)\Theta_1(B^{12}) &= (1-\theta_1 B)(1-\Theta_1 B^{12}) \\ &= 1-\theta_1 B-\Theta_1 B^{12}+\theta_1\Theta_1 B^{13}\end{aligned}$$

where $q = Q = 1$. In both equations, S denotes the seasonal period (e.g., 12 for monthly data where the data exhibit annual seasonality [7]).

More specifically, the SARFIMA$(1,d,1)\times(1,0,1)^{12}$ process with exponential white noise can be simplified as:

$$(1-\phi_1 B)(1-\Phi_1 B^{12})X_t = (1-\theta_1 B)(1-\Theta_1 B^S)(1-B)^{-d}\varepsilon_t \quad (2)$$

where $(1-B)^{-d}\varepsilon_t$ represents the fractionally integrated noise process applied in reverse (integration). Operator $(1-B)^{-d}$ can be expanded using a binomial (Maclaurin) series into an infinite weighted sum of backward-shift operators as follows:

$$\begin{aligned}(1-B)^{-d} &= \sum_{i=0}^{\infty}\pi_i B^i \\ &= 1+dB+\frac{d(d+1)}{2!}B^2+\frac{d(d+1)(d+2)}{3!}B^3+\ldots\end{aligned}$$

where coefficients π_i are defined using a Gamma function as $\pi_i = \frac{\Gamma(i+d)}{\Gamma(i+1)\Gamma(d)}$, $i = 0, 1, 2, \ldots$, and parameter d denotes the fractional differencing parameter that can take non-integer values (i.e., $0 < d < 0.5$). The latter governs the strength of the long-range dependence in the process [18].

In the present study, observations X_t generated from the SARFIMA$(1,d,1)\times(1,0,1)^{12}$ process with exponential white noise are used to construct the EWMA control chart as follows:

$$X_t = \left(\sum_{i=0}^{\infty}\pi_i B^i\right)\varepsilon_t - \left(\sum_{i=0}^{\infty}\pi_i B^i\right)\theta_1\varepsilon_{t-1} - \left(\sum_{i=0}^{\infty}\pi_i B^i\right)\Theta_1\varepsilon_{t-12} + \left(\sum_{i=0}^{\infty}\pi_i B^i\right)\theta_1\Theta_1\varepsilon_{t-12} + \phi_1 X_{t-1}B + \Phi_1 X_{t-12} - \phi_1\Phi_1 X_{t-13} \quad (3)$$

Next, the EWMA statistic can be constructed to monitor shifts in the process mean. The observed series X_t is assumed to follow a $\text{SARFIMA}(1,d,1)\times(1,0,1)^{12}$ process with exponential white noise, as specified in (3). The EWMA statistic can be defined recursively as:

$$Y_t = (1-\lambda)Y_{t-1} + \lambda X_t \quad (4)$$

with initial value $Y_0 = \psi$, representing the in-control mean $(0 < \psi < \hbar)$. The smoothing parameter $\lambda \in (0,1]$ controls the weighting of past observations: a larger λ value emphasizes recent data, whereas a smaller λ value assigns greater weight to historical observations. Interestingly, for a sufficiently small λ value, the EWMA control chart approaches CUSUM-type behavior [20].

The center line (CL), lower control limit (LCL), and upper control limit (UCL) are given by:

$$\text{CL} = \mu_0, \quad \text{LCL/ UCL} = \mu_0 \pm L\sigma\sqrt{\frac{\lambda}{2-\lambda}\left[1-(1-\lambda)^{2t}\right]} \quad (5)$$

where μ_0 and σ denote the process mean and standard deviation, respectively, and L is the EWMA design parameter.

III. MONITORING PROCEDURE

A. Numerical Integral Equation Method

The ARL is approximated using the NIE approach via four quadrature schemes: the composite midpoint, trapezoidal, Gauss–Legendre, and Simpson's rules. These schemes are applied to the EWMA control chart for a long-memory $\text{SARFIMA}(1,d,1)\times(1,0,1)^{12}$ process with exponential white noise. The computational efficiency and numerical stability of the solutions are compared to determine the most appropriate approximation method in this scenario.

Let $\mathcal{L}(\psi)$ denote the ARL of the upper one-sided EWMA control chart given the initial state (ψ). For a process following the $\text{SARFIMA}(1,d,1)\times(1,0,1)^{12}$ model, the ARL is defined as:

$$\text{ARL} = \mathcal{L}(\psi) = \mathbb{E}_{\infty}(\tau_{\hbar}) < \infty \quad (6)$$

where $\tau_{\hbar} = \inf\{t > 0;\ Z_t > \hbar\}$ is the stopping time at which the EWMA statistic first exceeds the UCL $(\hbar)$.

The function $\widetilde{\mathcal{L}(\psi)}$ satisfying the prerequisites for an integral equation forms the basis for the NIE approximation as follows:

$$\mathcal{L}(\psi) = 1 + \frac{1}{\lambda}\int_0^{\hbar}\mathcal{L}(y)\,\mathcal{K}(\psi, y)\,dy \quad (7)$$

where:

$$\mathcal{K}(\psi, y) = f\left(\frac{y-(1-\lambda)\psi}{\lambda} - \left(\sum_{i=0}^{\infty}\pi_i B^i\right)\varepsilon_t + \left(\sum_{i=0}^{\infty}\pi_i B^i\right)\theta_1\varepsilon_{t-1} + M\right)$$

and:

$$M = \left(\sum_{i=0}^{\infty}\pi_i B^i\right)\Theta_1\varepsilon_{t-12} - \left(\sum_{i=0}^{\infty}\pi_i B^i\right)\theta_1\Theta_1\varepsilon_{t-12} - \phi_1 X_{t-1}B - \Phi_1 X_{t-12} + \phi_1\Phi_1 X_{t-13}.$$

Subsequently, the integral equation can be transformed numerically:

$$f(\upsilon_j) = f\left(\frac{\upsilon_j-(1-\lambda)\upsilon_i}{\lambda} - \left(\sum_{i=0}^{\infty}\pi_i B^i\right)\varepsilon_t + \left(\sum_{i=0}^{\infty}\pi_i B^i\right)\theta_1\varepsilon_{t-1} + M\right)$$

The quadrature rule is applied by partitioning the interval $[0,\hbar]$ into $0 \le \upsilon_1 \le \upsilon_2 \le \cdots \le \upsilon_m \le \hbar$, where m denotes the number of nodes and ω_j are the associated constant weights. Rewriting (6) in discrete numerical form gives:

$$\widetilde{\mathcal{L}(\upsilon_j)} = 1 + \frac{1}{\lambda}\sum_{j=1}^{m}\omega_j\widetilde{\mathcal{L}(\upsilon_j)}f(\upsilon_j) \quad (8)$$

Applying a quadrature rule transforms the integral equation into a system of linear algebraic equations as follows:

$$\widetilde{\mathcal{L}(\upsilon_j)} \approx 1 + \frac{1}{\lambda}\sum_{j=1}^{m}\omega_j\widetilde{\mathcal{L}(\upsilon_j)}f\left(\frac{\upsilon_j-(1-\lambda)\upsilon_i}{\lambda} - \left(\sum_{i=0}^{\infty}\pi_i B^i\right)\varepsilon_t + \left(\sum_{i=0}^{\infty}\pi_i B^i\right)\theta_1\varepsilon_{t-1} + M\right)$$

Thus,

$$\widetilde{\mathcal{L}(\upsilon_1)} \approx 1 + \frac{1}{\lambda}\sum_{j=1}^{m}\omega_j\widetilde{\mathcal{L}(\upsilon_j)}f\left(\frac{\upsilon_j-(1-\lambda)\upsilon_1}{\lambda} - \left(\sum_{i=0}^{\infty}\pi_i B^i\right)\varepsilon_t + \left(\sum_{i=0}^{\infty}\pi_i B^i\right)\theta_1\varepsilon_{t-1} + M\right)$$

$$\widetilde{\mathcal{L}(\upsilon_2)} \approx 1 + \frac{1}{\lambda}\sum_{j=1}^{m}\omega_j\widetilde{\mathcal{L}(\upsilon_j)}f\left(\frac{\upsilon_j-(1-\lambda)\upsilon_2}{\lambda} - \left(\sum_{i=0}^{\infty}\pi_i B^i\right)\varepsilon_t + \left(\sum_{i=0}^{\infty}\pi_i B^i\right)\theta_1\varepsilon_{t-1} + M\right)$$

$$\vdots \qquad\qquad \vdots$$

$$\widetilde{\mathcal{L}(\upsilon_m)} \approx 1 + \frac{1}{\lambda}\sum_{j=1}^{m}\omega_j\widetilde{\mathcal{L}(\upsilon_j)}f\left(\frac{\upsilon_j-(1-\lambda)\upsilon_m}{\lambda} - \left(\sum_{i=0}^{\infty}\pi_i B^i\right)\varepsilon_t + \left(\sum_{i=0}^{\infty}\pi_i B^i\right)\theta_1\varepsilon_{t-1} + M\right)$$

These can be written in matrix form as:

$\mathbf{L}_{m\times1} = \mathbf{I}_m + \mathbf{R}_{m\times m}\mathbf{L}_{m\times1}$, or $(\mathbf{I}_m - \mathbf{R}_{m\times m})\mathbf{L}_{m\times1} = \mathbf{1}_{m\times1}$.

A column vector can be defined as $\mathbf{L}_{m\times1} = \left[\widetilde{\mathcal{L}(\upsilon_1)}, \widetilde{\mathcal{L}(\upsilon_2)}, ..., \widetilde{\mathcal{L}(\upsilon_m)}\right]'$.

We assume that $\mathbf{1}_{m\times1} = [1,1,...,1]'$ is an $m\times1$ vector of ones and $\mathbf{R}$ is a matrix in which the (i,j)-th entry is defined by:

$$[R_{ij}] \approx \frac{1}{\lambda}\omega_j f\left(\begin{array}{l}\dfrac{\upsilon_j - (1-\lambda)\upsilon_i}{\lambda} - \left(\sum_{i=0}^{\infty}\pi_i B^i\right)\varepsilon_t \\ + \left(\sum_{i=0}^{\infty}\pi_i B^i\right)\theta_1\varepsilon_{t-1} + M\end{array}\right)$$

Assuming that $\mathbf{I}_m$ is an identity matrix of order m, provided that $(\mathbf{I}_m - \mathbf{R}_{m\times m})^{-1}$ exists, the numerical solution for the integral equation can be written in matrix form as:

$$\mathbf{L}_{m\times1} = (\mathbf{I}_m - \mathbf{R}_{m\times m})^{-1}\mathbf{1}_{m\times1} \quad (9)$$

Finally, replacing υ_i with ψ in $\widetilde{\mathcal{L}(\upsilon_j)}$ yields the numerical approximation of the ARL function as follows:

$$\widetilde{\mathcal{L}(\psi)} \approx 1 + \frac{1}{\lambda}\sum_{j=1}^{m}\omega_j\widetilde{\mathcal{L}(\upsilon_j)}f\left(\begin{array}{l}\dfrac{\upsilon_j - (1-\lambda)\psi}{\lambda} - \left(\sum_{i=0}^{\infty}\pi_i B^i\right)\varepsilon_t \\ + \left(\sum_{i=0}^{\infty}\pi_i B^i\right)\theta_1\varepsilon_{t-1} + M\end{array}\right)$$

The ARL was approximated via the NIE method using the Gauss–Legendre quadrature rule ($\widetilde{\mathcal{L}_G(\psi)}$). For comparison, the composite midpoint, trapezoidal, and Simpson rules were also applied to approximate the ARL, for which the various choices of nodes and weights in the integral formulation are summarized in Table I.

TABLE I. NODES AND WEIGHTS FOR THE COMPOSITE MIDPOINT, TRAPEZOIDAL, AND SIMPSON QUADRATURE RULES FOR ARL COMPUTATION

NIE method	Nodes υ_j	Weights ω_j
Midpoint rule $\left(\widetilde{\mathcal{L}_M(\psi)}\right)$	$\hbar/m\,(j-0.5)$	$\hbar/m;\ j=1,2,...,m$
Trapezoidal rule $\left(\widetilde{\mathcal{L}_T(\psi)}\right)$	$j\omega_j$	$\hbar/m;\ j=1,2,...,m-1$ $\hbar/2m;\ j=$ otherwise
Simpson rule $\left(\widetilde{\mathcal{L}_S(\psi)}\right)$	$j\omega_j$	$4/3(\hbar/2m);\ j=1,3,...,2m-1$ $2/3(\hbar/2m);\ j=2,4,...,2m-2$ $1/3(\hbar/2m);\ j=$ otherwise

B. Run-Length Metrics

1) Standard Deviation of the Run Length

The integral equations in (7), corresponding to the first and second moments [21, 22], can be rewritten as:

$$\mathcal{H}(\psi) = 1 + 2\frac{1}{\lambda}\int_0^{\hbar}\mathcal{L}(y)\mathcal{K}(\psi,y)dy + \int_0^{\hbar}\mathcal{H}(y)\mathcal{K}(\psi,y)dy \quad (10)$$

or in matrix form as: $(\mathbf{I}_m - \mathbf{R}_{m\times m})\mathbf{H}_{m\times1} = 2\mathbf{L}_{m\times1} - \mathbf{1}_{m\times1}$.

Solving the resulting linear equation system yields the first and second moments of the run-length distribution, from which the SDRL is obtained:

$$\text{SDRL} = \sqrt{\mathcal{H}(\psi) - \mathcal{L}(\psi)^2}.$$

2) Run-Length Quartiles

Let $\tau_{\hbar}$ denote the run length of the EWMA control chart and let $F_{\tau_{\hbar}}(r) = 1 - e^{-r/ARL}$ be its cumulative distribution function, which is approximated by an exponential distribution. Solving $F_{\tau_{\hbar}}(r) = p$ yields the p-th quantile as follows:

$$\text{MRL}_p = -\mathcal{L}(\psi)ln(1-p).$$

Specifically, the Median Run Length (MRL) values MRL25, MRL50 (median), and MRL75 correspond to the 1st, 2nd, and 3rd quartiles of the run-length distribution (RLQ1, RLQ2, and RLQ3), respectively.

These quartiles reflect the variability and skewness of the run length. While the ARL measures the mean detection delay, the median and quartiles comprise a more informative performance measure, especially since the EWMA run-length distribution is typically right-skewed.

IV. NUMERICAL RESULTS

A. In-Control Performance Evaluation

To determine the control limit ($\hbar$) that yields a desired ARL value, the proposed algorithm was applied under In-Control (IC) conditions ($\delta = 0$). Table II reports the resulting control limits for smoothing parameter λ = 0.05, 0.10, and 0.15, corresponding to the target ARL0 = 370 for a long-memory SARFIMA$(1,d,1)\times(1,D,1)^{12}$ process with exponential white noise. These λ values were selected based on commonly recommended ranges in the EWMA literature [4] (0.05–0.20), as smaller λ enhances sensitivity to small and persistent shifts, particularly in long-memory and serially dependent processes, consistent with previous studies. For a fixed ARL0, a larger smoothing parameter value required a smaller control limit value.

For example, under the long-memory SARFIMA$(1,d,1)\times(1,D,1)^{12}$ model with exponential white noise, with parameter settings $\phi_1 = \theta_1 = \Phi_1 = \Theta_1 = 0.1$ and $d = 0.1$, the obtained control limits were $\hbar$ = 0.000000013157, 0.000555849, and 0.01090883 for λ = 0.05, 0.10, and 0.15, respectively.

Table I (Appendix) shows that when the process was IC, the control chart produced ARL0 ≈ 370 for all λ, values, which indicates proper calibration of the control limits and a stable false-alarm rate. The relatively large SDRL and wide

interquartile range (MRL25 = 106, MRL50 = 256, MRL75 = 513) reflect the inherent variability of the run-length distribution under IC conditions.

TABLE II. CONTROL LIMITS FOR THE EWMA CONTROL CHART WITH VARIOUS λ VALUES FOR LONG-MEMORY SARFIMA$(1,d,1)\times(1,D,1)^{12}$ MODELS WITH EXPONENTIAL WHITE NOISE AND $ARL_0 = 370$

Parameters of SARFIMA$(1,d,1)\times(1,D,1)^{12}$						λ		
Model	ϕ_1	d	θ_1	Φ_1	Θ_1	**0.05**	**0.10**	**0.15**
[1]	0.1	0.1	0.1	0.1	0.1	0.000000013157	0.0005558490	0.01090883
[2]	-0.1	0.1	0.1	0.1	0.1	0.000000015425	0.0006519615	0.01283113
[3]	0.1	0.2	0.1	0.1	0.1	0.000000012289	0.0005187195	0.01017000
[4]	-0.1	0.2	0.1	0.1	0.1	0.000000014103	0.0005958500	0.01170750
[5]	0.1	0.4	0.1	0.1	0.1	0.000000010815	0.0004566989	0.00893740
[6]	-0.1	0.4	0.1	0.1	0.1	0.0000000119278	0.0005037950	0.00987225

B. Out-of-Control Performance Evaluation

To evaluate the Out-of-Control (OOC) performance of the EWMA control chart, combinations of the design parameters $(\lambda, \hbar)$ listed in Table II were considered. Mean shifts δ = 0.15, 0.30, 0.45, 0.60, 0.75, and 0.90 (expressed in units of the process standard deviation) were examined. Values for the zero-state run-length metrics (ARL, SDRL, and RLQs) were obtained under a nominal IC ARL of approximately 370. Table I (Appendix) reports the run-length performance of the proposed EWMA scheme in terms of the ARL, SDRL, and RLQs 1 to 3 (MRL25, MRL50, and MRL75), respectively, across various shift magnitudes and smoothing parameter values.

As the shift magnitude increased (i.e., $\delta > 0$), the ARL decreased rapidly, thereby indicating faster detection of process mean changes. The SDRL and all RLQs also declined, reflecting both improved detection speed and more consistent signaling. For moderate-to-large process mean shifts (i.e., $0.15 < \delta \le 2.00$), the ARL approached 1–3, thereby implying near-immediate signaling of the OOC state. The SDRL and RLQs decreased concurrently, showing reduced variability as the process mean shift was increased.

The magnitude of the smoothing parameter λ strongly affected the detection performance. Smaller values (e.g., $\lambda = 0.05$) yielded lower ARLs for small-to-moderate process mean shifts, whereas larger values ($\lambda = 0.10$, $\lambda = 0.15$) produced higher ARLs, indicating slower detection but smoother monitoring statistics for each model.

Overall, the ARL approximations via the NIE method with the four numerical integration rules provided nearly identical results. The proposed EWMA control chart effectively detected process mean shifts, particularly small ones. In terms of the RLQ results describing variability in the run-length distribution, smaller λ values led to earlier detection of minor shifts in the process mean.

Considering the results in Table II (Appendix), the four NIE methods yielded numerically indistinguishable ARL approximations, indicating that accuracy was largely insensitive to the choice of integration rule. The primary difference lay in computational efficiency: Gauss–Legendre quadrature exhibited the highest computational burden (7–8 s), followed by Simpson's rule (5–6 s) and finally the midpoint and trapezoidal rules (1.4–1.5 s), the latter two achieving substantially lower computational times.

From a statistical perspective, these results demonstrate that higher-order quadrature in the NIE formulation does not provide a meaningful gain in estimation precision for the ARL. Consequently, the midpoint rule offers the most favorable balance between computational cost and numerical accuracy and is therefore recommended for practical applications.

V. PRACTICAL IMPLEMENTATION

An empirical analysis was conducted on a monthly XAU/USD (spot gold price in US dollars) series from January 2020 to February 2026 [23]. The fitted SARFIMA$(1,d,1)\times(1,D,1)^{12}$ model could adequately represent the data (Table III).

TABLE III. ESTIMATED COEFFICIENTS FOR THE SARFIMA(1, *D,* 1)(1, 0, 1)^{12} MODEL APPLIED TO THE XAU/USD MONTHLY GOLD PRICE SERIES

Variable	**Coefficient**	**Std. error**	**t-statistic**	**p-value**
AR(1)	0.999996	0.062	16.184	0.000*
d	0.459338	0.040	11.343	0.000*
MA(1)	−0.329902	0.047	−6.993	0.000*
SAR(12)	−0.288014	0.025	−11.421	0.000*
SMA(12)	0.999778	0.083	12.002	0.000*
Akaike Info Criterion (AIC)				12.6273
Schwarz Bayesian Information Criterion (BIC)				12.7830
Hannan-Quinn Criterion (HQ)				12.6894
Durbin-Watson				1.9530

All estimated parameters were statistically significant at the 5% level. The fractional differencing parameter $\hat{d}$ = 0.459338 (t = 11.343), lies within $0 < \hat{d} < 0.5$, thus indicating covariance-stationary long-memory behavior. The AR(1) coefficient value of 0.999996 implies strong persistence, whereas the MA(1) coefficient value of −0.329902 indicates partial correction of short-term shocks. The values of the seasonal terms (SAR(12) = -0.288014 and SMA(12) = 0.999778) confirm annual seasonality in the monthly series. The results for various criteria support the model's adequacy (AIC = 12.6273, BIC = 12.7830, HQ = 12.6894), indicating a parsimonious specification, whereas the Durbin–Watson statistic (1.953) failed to reveal any residual serial correlation. Hence, the SARFIMA$(1,0.4593,1)\times(1,0,1)^{12}$ model was considered suitable for the subsequent monitoring analysis.

The results in Table IV reveal that the assumption that the white noise is exponentially distributed is correct: the residual mean (81.7988) corresponds to an exponential rate estimate $\hat{\alpha} = 0.0122$, whereas applying the Anderson–Darling test (0.8284, p-value = 0.4602) failed to reject the exponential distribution at the 5% level.

The diagnostic results in Figure 1 support the assumption that the white noise was exponentially distributed: the

histogram in Figure 1(a) exhibits the characteristic right-skewness of an exponential distribution, whereas the exponential Q–Q plot in Figure 1(b) is approximately linear with only minor tail departures. As the model captures both seasonal and long-memory dependence, it facilitates accurate ARL approximation under the NIE method for EWMA control chart analysis. Since all four methods yield essentially identical and highly accurate ARL estimates, only a single representative column is displayed in Table III (Appendix) for brevity. In addition, the computed SDRL and RLQs (MRL_{25}, MRL_{50}, and MRL_{75}) exhibit patterns consistent with the simulation results reported in Table III (Appendix).

TABLE IV. SUITABILITY OF THE EXPONENTIAL DISTRIBUTION FOR THE RESIDUAL (EXPONENTIAL WHITE NOISE) SERIES

Exponential white noise		**Estimate**
Mean of residuals		81.7988
Exponential rate parameter		0.0122
Goodness of fit	**Statistic**	**p-value**
Anderson–Darling	0.8284	0.4602 [ns]

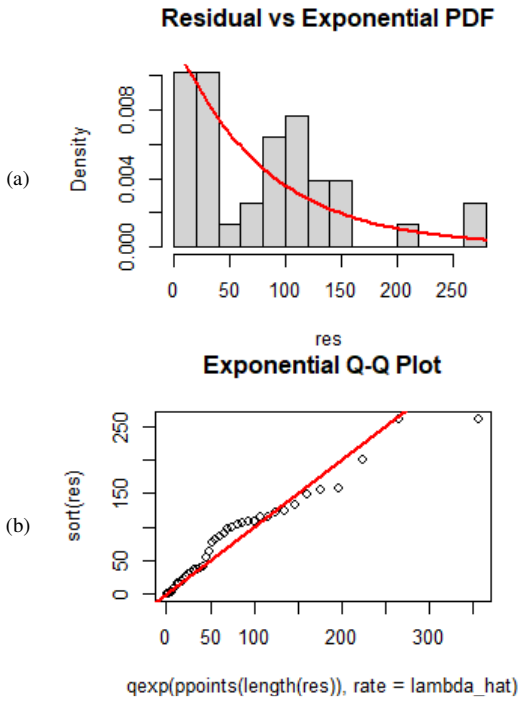

Fig. 1. Graphical representation of the residuals from the fitted $SARFIMA(1,0.4593,1)\times(1,0,1)^{12}$ model: (a) a histogram with fitted exponential density, and (b) an exponential Q–Q plot.

IC performance: With ARL_0 calibrated at 370, the SDRL (443.560) significantly exceeds the ARL, confirming a highly right-skewed run length distribution. The MRL_{50} of 256 suggests that 50% of false alarms occur much earlier than the mean ARL, highlighting that MRL is a more realistic indicator for practitioners than ARL alone.

OOC performance: The chart demonstrates high sensitivity to process shifts. As the shift magnitude increases, the ARL drops sharply from 370 to 1. The MRL_{50} values confirm that the chart reliably detects most shifts within 1–5 observations. These findings strongly support the recommendation by authors in [24] that relying solely on the ARL metric can be misleading, and reporting the MRL provides a more realistic representation of the chart's performance for practitioners.

The computational times for the four NIE-based methods are summarized in Table IV (Appendix), where the composite midpoint and trapezoidal rules require comparably low execution times. The close agreement between the numerical and simulation results (see Table II (Appendix)) further confirms the accuracy of the NIE approach.

Overall, these findings provide strong empirical evidence for the validity of all four quadrature schemes. Considering both numerical accuracy and computational efficiency, the composite midpoint rule is recommended for practical implementation in the monitoring scenario outlined in this study.

VI. CONCLUSIONS AND RECOMMENDATIONS

An analytical evaluation of the Exponentially Weighted Moving Average (EWMA) control chart was developed based on the Numerical Integral Equation (NIE) method for seasonal long-memory processes with exponential white noise. In this NIE approach, the Fredholm integral equation of the second kind was transformed into a numerical form and solved using several quadrature rules (Gauss–Legendre quadrature, midpoint, trapezoidal, and Simpson's). Moreover, the analytical approach provides direct approximates of run-length characteristics without relying on extensive Monte Carlo simulation.

The EWMA control chart attained the target In-Control (IC) performance (ARL_0 = 370), thereby confirming proper calibration of the control limits. As the shift magnitude was increased, the Average Run Length (ARL) decreased rapidly, indicating effective Out-of-Control (OOC) detection. The values of the Standard Deviation of the Run Length (SDRL) and the Run-Length Quartiles (RLQs), namely RLQ1, RLQ2, and RLQ3, also declined, reflecting fast and stable signaling performance. The smoothing parameter λ was found to strongly influence sensitivity: smaller λ values improved detection of small-to-moderate shifts, whereas larger λ values yielded smoother statistics but a slower response. Hence, a small λ value is recommended when early detection of process mean shifts is required.

Although all four quadrature rules under the NIE method produced identical and accurate ARL approximations, their computational efficiencies differed. The midpoint and trapezoidal rules offer the best balance between speed and numerical stability, whereas the Gauss–Legendre rule requires longer computation time without accuracy gains. Accordingly, the midpoint (or trapezoidal) rule is recommended for practical implementation.

The proposed approach can be extended to multivariate monitoring (e.g., MEWMA), adaptive EWMA schemes with dynamically adjusted smoothing parameters, and time-varying EWMA schemes to address non-stationarity. It is also applicable to other long-memory or non-Gaussian processes.

Further study under model misspecification and integration into real-time industrial monitoring systems would enhance its practical applicability.

DECLARATION OF COMPETING INTERESTS

Not applicable to this work.

ACKNOWLEDGMENT

This research budget was allocated by National Science, Research and Innovation Fund (NSRF) and King Mongkut's University of Technology North Bangkok under contract no. KMUTNB-FF-69-B-32.

DATA AVAILABILITY

Not applicable to this work.

REFERENCES

[1] D. C. Montgomery, *Introduction to Statistical Quality Control*, 8th ed. Hoboken, NJ, USA: Wiley, 2019.

[2] S. W. Roberts, "Control Chart Tests Based on Geometric Moving Averages," *Technometrics*, vol. 1, no. 3, pp. 239–250, Aug. 1959, https://doi.org/10.1080/00401706.1959.10489860.

[3] E. S. PAGE, "Continuous Inspection Schemes," *Biometrika*, vol. 41, no. 1–2, pp. 100–115, June 1954, https://doi.org/10.1093/biomet/41.1-2.100.

[4] S. H. Steiner, "EWMA Control Charts with Time-Varying Control Limits and Fast Initial Response," *Journal of Quality Technology*, vol. 31, no. 1, pp. 75–86, Jan. 1999, https://doi.org/10.1080/00224065.1999.11979899.

[5] N. Abbas, M. Riaz, and R. J. M. M. Does, "An EWMA-Type Control Chart for Monitoring the Process Mean Using Auxiliary Information," *Communications in Statistics - Theory and Methods*, vol. 43, no. 16, pp. 3485–3498, Aug. 2014, https://doi.org/10.1080/03610926.2012.700368.

[6] M. Awais and A. Haq, "An EWMA chart for monitoring process mean," *Journal of Statistical Computation and Simulation*, vol. 88, no. 5, pp. 1003–1025, Mar. 2018, https://doi.org/10.1080/00949655.2017.1421193.

[7] C. W. J. Granger and R. Joyeux, "An Introduction to Long-Memory Time Series Models and Fractional Differencing," *Journal of Time Series Analysis*, vol. 1, no. 1, pp. 15–29, 1980, https://doi.org/10.1111/j.1467-9892.1980.tb00297.x.

[8] J. R. M. Hosking, "Fractional differencing," *Biometrika*, vol. 68, no. 1, pp. 165–176, Apr. 1981, https://doi.org/10.1093/biomet/68.1.165.

[9] J. Beran, *Statistics for Long-Memory Processes*. Boca Raton, FL, USA: Chapman and Hall/CRC, 1994, https://doi.org/10.1201/9780203738481.

[10] L. Rabyk and W. Schmid, "EWMA control charts for detecting changes in the mean of a long-memory process," *Metrika*, vol. 79, no. 3, pp. 267–301, Apr. 2016, https://doi.org/10.1007/s00184-015-0555-7.

[11] R. T. Baillie, "Long memory processes and fractional integration in econometrics," *Journal of Econometrics*, vol. 73, no. 1, pp. 5–59, July 1996, https://doi.org/10.1016/0304-4076(95)01732-1.

[12] W. Palma, *Long-Memory Time Series: Theory and Methods*, 1st ed. Hoboken, NJ, USA: Wiley, 2006, https://doi.org/10.1002/9780470131466.

[13] I. M. S. Pereira and M. Antonia Amaral-Turkman, "Bayesian prediction in threshold autoregressive models with exponential white noise," *Test*, vol. 13, no. 1, pp. 45–64, June 2004, https://doi.org/10.1007/BF02603000.

[14] P. A. Jacobs and P. a. W. Lewis, "A mixed autoregressive-moving average exponential sequence and point process (EARMA 1,1)," *Advances in Applied Probability*, vol. 9, no. 1, pp. 87–104, Mar. 1977, https://doi.org/10.2307/1425818.

[15] Suparman, "A New Estimation Procedure Using a Reversible Jump MCMC Algorithm for AR Models of Exponential White Noise," *International Journal of GEOMATE*, vol. 15, no. 49, pp. 85–91, Sept. 2018, https://doi.org/10.21660/2018.49.3622.

[16] C. W. Champ and S. E. Rigdon, "A a comparison of the markov chain and the integral equation approaches for evaluating the run length distribution of quality control charts," *Communications in Statistics - Simulation and Computation*, vol. 20, no. 1, pp. 191–204, Jan. 1991, https://doi.org/10.1080/03610919108812948.

[17] S. V. Crowder, "Average Run Lengths of Exponentially Weighted Moving Average Control Charts," *Journal of Quality Technology*, vol. 19, no. 3, pp. 161–164, July 1987, https://doi.org/10.1080/00224065.1987.11979055.

[18] Y. Areepong and W. Peerajit, "Enhancing the Detection Power of CUSUM Charts for Changes in the Mean of the Long-Memory ARFIMAX Model with Exponential White Noise," *Engineering, Technology & Applied Science Research*, vol. 15, no. 6, pp. 29103–29112, Dec. 2025, https://doi.org/10.48084/etasr.13174.

[19] P. Phanthuna and Y. Areepong, "Change-Detected ARIMA (1,1,1) Time Series Using the Approximated and Exact ARL of the MEWMA Scheme," *Malaysian Journal of Fundamental and Applied Sciences*, vol. 22, no. 1, pp. 215–233, Feb. 2026, https://doi.org/10.11113/mjfas.v22n1.4907.

[20] J. S. Hunter, "The Exponentially Weighted Moving Average," *Journal of Quality Technology*, vol. 18, no. 4, pp. 203–210, Oct. 1986, https://doi.org/10.1080/00224065.1986.11979014.

[21] D. Brook and D. A. Evans, "An approach to the probability distribution of cusum run length," *Biometrika*, vol. 59, no. 3, pp. 539–549, Dec. 1972, https://doi.org/10.1093/biomet/59.3.539.

[22] C. Li, S. Cui, and D. Wang, "Monitoring the Zero-Inflated Time Series Model of Counts with Random Coefficient," *Entropy*, vol. 23, no. 3, Mar. 2021, Art. no. 372, https://doi.org/10.3390/e23030372.

[23] "XAU/USD - Gold Spot US Dollar Historical Data." Investing. https://www.investing.com/currencies/xau-usd-historical-data.

[24] S. Chakraborti, "Run Length Distribution and Percentiles: The Shewhart Chart with Unknown Parameters," *Quality Engineering*, vol. 19, no. 2, pp. 119–127, Apr. 2007, https://doi.org/10.1080/08982110701276653.

APPENDIX

TABLE I. ARL APPROXIMATION METHODS FOR THE EWMA CONTROL CHART WITH A × SARFIMA(1, *D*, 1)(1, 0,1)^{12} MODEL WHEN $ARL_0 = 370$

Model	δ	λ = 0.05					λ = 0.10					λ = 0.15				
		ARL 4 NIE	SDRL	MRL25	MRL50	MRL75	ARL	SDRL	MRL25	MRL50	MRL75	ARL	SDRL	MRL25	MRL50	MRL75
[1]	0.00	370.000	369.5 δ 00	106	256	513	370.001	369.501	106	256	513	370.000	369.500	106	256	513
	0.15	21.571	21.065	6	15	30	75.695	75.194	22	52	105	82.650	82.148	24	57	115
	0.30	3.199	2.653	1	2	4	22.605	22.099	7	16	31	29.526	29.022	8	20	41
	0.45	1.369	0.711	0	1	2	8.994	8.479	3	6	12	13.732	13.222	4	10	19
	0.60	1.086	0.305	0	1	2	4.532	4.001	1	3	6	7.658	7.140	2	5	11
	0.75	1.025	0.161	0	1	1	2.782	2.226	1	2	4	4.893	4.364	1	3	7
	0.90	1.009	0.095	0	1	1	1.995	1.409	1	1	3	3.473	2.930	1	2	5
[2]	0.00	370.000	369.499	106	256	513	370.000	369.500	106	256	513	370.000	369.500	106	256	513

Model	δ	λ = 0.05					λ = 0.10					λ = 0.15				
		ARL 4 NIE	SDRL	MRL25	MRL50	MRL75	ARL	SDRL	MRL25	MRL50	MRL75	ARL	SDRL	MRL25	MRL50	MRL75
	0.15	22.003	21.497	6	15	31	77.313	76.811	22	54	107	85.377	84.875	25	59	118
	0.30	3.281	2.736	1	2	5	23.432	22.927	7	16	32	30.994	30.489	9	21	43
	0.45	1.388	0.733	0	1	2	9.406	8.892	3	7	13	14.550	14.041	4	10	20
	0.60	1.091	0.315	0	1	2	4.753	4.223	1	3	7	8.152	7.636	2	6	11
	0.75	1.027	0.167	0	1	1	2.909	2.357	1	2	4	5.214	4.687	2	4	7
	0.90	1.010	0.099	0	1	1	2.074	1.492	1	1	3	3.694	3.154	1	3	5
[3]	0.00	370.000	369.757	107	257	513	370.000	369.501	106	256	513	370.000	369.573	106	257	513
	0.15	21.404	20.895	6	15	30	75.069	74.503	22	52	104	81.610	81.014	23	57	113
	0.30	3.168	2.619	1	2	4	22.288	21.750	6	15	31	28.974	28.417	8	20	40
	0.45	1.362	0.701	0	1	2	8.837	8.306	3	6	12	13.426	12.887	4	9	19
	0.60	1.084	0.301	0	1	2	4.449	3.909	1	3	6	7.474	6.939	2	5	10
	0.75	1.025	0.159	0	1	1	2.734	2.172	1	2	4	4.774	4.233	1	3	7
	0.90	1.009	0.094	0	1	1	1.965	1.374	1	1	3	3.391	2.840	1	2	5
[4]	0.00	370.000	369.551	106	257	513	370.000	369.507	106	256	513	370.000	369.509	106	256	513
	0.15	21.775	21.255	6	15	30	76.460	75.895	22	53	106	76.460	83.323	24	58	116
	0.30	3.238	2.689	1	2	4	22.994	22.456	7	16	32	22.994	29.650	9	21	42
	0.45	1.378	0.721	0	1	2	9.187	8.656	3	6	13	9.187	13.571	4	10	20
	0.60	1.088	0.309	0	1	2	4.635	4.096	1	3	6	4.635	7.351	2	5	11
	0.75	1.026	0.164	0	1	1	2.841	2.282	1	2	4	2.841	4.502	1	3	7
	0.90	1.009	0.097	0	1	1	2.031	1.444	1	1	3	2.031	3.025	1	2	5
[5]	0.00	370.000	369.500	106	256	513	370.000	369.500	106	256	513	370.000	369.530	106	256	513
	0.15	21.052	20.546	6	15	29	73.751	73.249	21	51	102	79.456	78.955	23	55	110
	0.30	3.102	2.554	1	2	4	21.628	21.122	6	15	30	27.842	27.338	8	19	39
	0.45	1.347	0.684	0	1	2	8.513	7.998	2	6	12	12.805	12.294	4	9	18
	0.60	1.080	0.293	0	1	1	4.278	3.745	1	3	6	7.103	6.584	2	5	10
	0.75	1.023	0.154	0	1	1	2.636	2.077	1	2	4	4.535	4.004	1	3	6
	0.90	1.008	0.091	0	1	1	1.906	1.314	1	1	3	3.228	2.681	1	2	4
[6]	0.00	370.000	369.499	106	256	513	370.000	369.500	106	256	513	370.000	369.499	106	256	513
	0.15	21.310	20.804	6	15	30	74.715	74.214	21	52	104	81.028	80.526	23	56	112
	0.30	3.150	2.602	1	2	4	22.110	21.604	6	15	31	28.667	28.162	8	20	40
	0.45	1.358	0.697	0	1	2	8.750	8.234	3	6	12	13.257	12.747	4	9	18
	0.60	1.083	0.299	0	1	2	4.403	3.870	1	3	6	7.373	6.855	2	5	10
	0.75	1.024	0.158	0	1	1	2.707	2.150	1	2	4	4.709	4.179	1	3	7
	0.90	1.009	0.093	0	1	1	1.949	1.360	1	1	3	3.346	2.802	1	2	5

TABLE II. COMPUTATION TIMES FOR THE ARL APPROXIMATIONS VIA THE NIE METHOD USING FOUR NUMERICAL INTEGRATION RULES: MIDPOINT, TRAPEZOIDAL, GAUSS–LEGENDRE QUADRATURE, AND SIMPSON'S.

Model	δ	λ = 0.05				λ = 0.10				λ = 0.15			
		$\widetilde{\mathcal{L}_M(\psi)}$	$\widetilde{\mathcal{L}_T(\psi)}$	$\widetilde{\mathcal{L}_G(\psi)}$	$\widetilde{\mathcal{L}_S(\psi)}$	$\widetilde{\mathcal{L}_M(\psi)}$	$\widetilde{\mathcal{L}_T(\psi)}$	$\widetilde{\mathcal{L}_G(\psi)}$	$\widetilde{\mathcal{L}_S(\psi)}$	$\widetilde{\mathcal{L}_M(\psi)}$	$\widetilde{\mathcal{L}_T(\psi)}$	$\widetilde{\mathcal{L}_G(\psi)}$	$\widetilde{\mathcal{L}_S(\psi)}$
[1]	0.150	1.484	1.454	8.016	5.282	1.485	1.500	8.031	5.906	1.500	1.562	8.016	6.109
	0.300	1.469	1.500	7.937	5.891	1.516	1.500	8.031	5.953	1.500	1.578	7.969	5.984
	0.450	1.421	1.516	8.047	5.781	1.485	1.500	8.000	5.891	1.468	1.485	7.953	6.079
	0.600	1.484	1.532	7.891	5.750	1.453	1.484	7.891	6.062	1.500	1.547	8.000	6.125
	0.750	1.437	1.469	8.141	5.781	1.500	1.468	8.094	6.156	1.500	1.578	7.891	6.047
	0.900	1.531	1.438	8.078	5.719	1.453	1.484	8.031	6.235	1.531	1.484	8.016	6.204
[2]	0.150	1.484	1.500	7.937	5.843	1.484	1.499	7.953	5.985	1.468	1.469	7.555	5.953
	0.300	1.484	1.516	7.937	5.859	1.500	1.516	7.922	5.921	1.469	1.531	7.867	5.781
	0.450	1.469	1.531	8.031	5.890	1.469	1.531	7.860	5.859	1.500	1.532	7.985	5.922
	0.600	1.469	1.500	8.343	5.797	1.453	1.484	8.005	5.765	1.500	1.500	8.005	5.875
	0.750	1.484	1.500	7.922	5.828	1.485	1.469	8.034	5.703	1.453	1.500	8.167	5.844
	0.900	1.516	1.453	8.250	5.843	1.484	1.500	8.068	5.797	1.468	1.531	7.945	5.687
[3]	0.150	1.485	1.495	8.156	5.844	1.500	1.492	8.579	5.685	1.485	1.500	7.938	5.845
	0.300	1.435	1.500	8.078	5.685	1.422	1.486	7.969	5.851	1.511	1.499	7.969	5.921
	0.450	1.500	1.465	8.120	5.789	1.557	1.500	9.610	6.312	1.489	1.475	8.032	5.789
	0.600	1.515	1.500	8.078	5.513	1.428	1.444	8.422	5.785	1.471	1.500	7.938	5.618
	0.750	1.495	1.500	8.094	5.752	1.435	1.585	7.937	5.666	1.491	1.517	7.937	5.788
	0.900	1.445	1.465	8.000	6.128	1.500	1.455	8.312	5.876	1.500	1.489	7.968	6.000
[4]	0.150	1.422	1.488	8.359	5.952	1.472	1.498	8.078	5.059	1.472	1.498	8.078	5.059
	0.300	1.497	1.521	8.250	5.872	1.444	1.487	8.031	6.128	1.444	1.487	8.031	6.128
	0.450	1.487	1.500	7.922	5.000	1.504	1.521	8.047	5.852	1.504	1.521	8.047	5.852
	0.600	1.517	1.500	7.922	6.422	1.487	1.489	7.938	5.789	1.487	1.489	7.938	5.789
	0.750	1.482	1.497	8.109	5.752	1.500	1.472	8.188	5.752	1.500	1.472	8.188	5.752
	0.900	1.444	1.488	8.062	5.118	1.488	1.506	7.984	6.185	1.488	1.506	7.984	6.185
[5]	0.150	1.487	1.500	7.978	5.911	1.079	1.316	6.235	5.078	1.078	1.478	6.391	5.297

Model	δ	λ = 0.05				λ = 0.10				λ = 0.15			
		$\widetilde{\mathcal{L}_M(\psi)}$	$\widetilde{\mathcal{L}_T(\psi)}$	$\widetilde{\mathcal{L}_G(\psi)}$	$\widetilde{\mathcal{L}_S(\psi)}$	$\widetilde{\mathcal{L}_M(\psi)}$	$\widetilde{\mathcal{L}_T(\psi)}$	$\widetilde{\mathcal{L}_G(\psi)}$	$\widetilde{\mathcal{L}_S(\psi)}$	$\widetilde{\mathcal{L}_M(\psi)}$	$\widetilde{\mathcal{L}_T(\psi)}$	$\widetilde{\mathcal{L}_G(\psi)}$	$\widetilde{\mathcal{L}_S(\psi)}$
	0.300	1.458	1.478	8.148	6.000	1.093	1.347	6.235	5.125	1.063	1.509	6.458	5.469
	0.450	1.478	1.497	7.489	6.152	1.078	1.331	6.250	5.266	1.016	1.431	6.484	5.343
	0.600	1.488	1.500	7.925	5.752	1.047	1.394	6.234	5.375	1.109	1.479	6.438	5.204
	0.750	1.500	1.512	8.474	5.965	1.078	1.378	6.390	5.203	1.011	1.525	6.781	5.250
	0.900	1.498	1.476	8.147	5.485	1.062	1.362	6.406	5.359	1.062	1.431	6.640	5.391
[6]	0.150	1.094	1.411	5.375	5.266	1.078	1.347	5.453	5.172	1.032	1.532	6.250	5.078
	0.300	1.062	1.493	5.390	5.375	1.063	1.378	6.328	5.313	1.094	1.578	6.235	5.391
	0.450	1.109	1.416	5.563	5.344	1.031	1.379	5.375	5.515	1.093	1.499	6.375	5.265
	0.600	1.062	1.446	5.406	5.438	1.063	1.347	5.922	5.439	1.094	1.563	6.140	6.141
	0.750	1.110	1.411	5.359	6.163	1.094	1.315	5.516	5.436	1.078	1.579	6.422	5.219
	0.900	1.078	1.463	5.422	5.536	1.031	1.362	5.687	5.434	1.093	1.531	6.328	5.281

TABLE III. APPROXIMATED ARL VALUES FOR THE PRACTICAL APPLICATION OF THE EWMA CONTROL CHART WITH THE SARFIMA(1, 0.4593, 1) × (1, 0, 1)^{12} MODEL WITH IN-CONTROL ARL_0 = 370

δ	λ = 0.05, $\hbar$ = 4.0297805					λ = 0.10, $\hbar$ = 8.4077844					λ = 0.15, $\hbar$ = 12.9603535				
	ARL 4 NIE	**SDRL**	**MRL25**	**MRL50**	**MRL75**	**ARL**	**SDRL**	**MRL25**	**MRL50**	**MRL75**	**ARL**	**SDRL**	**MRL25**	**MRL50**	**MRL75**
0.00	370.000	443.560	106	256	513	370.000	484.2562	106	256	513	370.000	493.981	106	256	513
0.15	6.4922	6.049	2	5	9	6.141	6.159	2	4	9	6.170	6.322	2	4	9
0.30	3.815	2.813	1	3	5	3.662	2.893	1	3	5	3.683	2.982	1	3	5
0.45	2.909	1.702	1	2	4	2.820	1.773	1	2	4	2.838	1.837	1	2	4
0.60	2.451	1.126	1	2	3	2.393	1.193	1	2	3	2.409	1.246	1	2	3
0.75	2.174	0.757	1	2	3	2.133	0.825	1	1	3	2.148	0.872	1	1	3
0.90	1.988	0.478	1	1	3	1.958	0.555	1	1	3	1.971	0.600	1	1	3

TABLE IV. COMPUTATION TIME (S) FOR APPROXIMATED ARL VIA THE NIE METHOD USING PRACTICAL IMPLEMENTATION

δ	λ = 0.05, $\hbar$ = 4.0297805				λ = 0.10, $\hbar$ = 8.4077844				λ = 0.15, $\hbar$ = 12.9603535			
	$\widetilde{\mathcal{L}_M(\psi)}$	$\widetilde{\mathcal{L}_T(\psi)}$	$\widetilde{\mathcal{L}_G(\psi)}$	$\widetilde{\mathcal{L}_S(\psi)}$	$\widetilde{\mathcal{L}_M(\psi)}$	$\widetilde{\mathcal{L}_T(\psi)}$	$\widetilde{\mathcal{L}_G(\psi)}$	$\widetilde{\mathcal{L}_S(\psi)}$	$\widetilde{\mathcal{L}_M(\psi)}$	$\widetilde{\mathcal{L}_T(\psi)}$	$\widetilde{\mathcal{L}_G(\psi)}$	$\widetilde{\mathcal{L}_S(\psi)}$
0.00	1.156	1.094	6.343	4.422	1.078	1.078	6.312	5.828	1.110	1.078	6.219	5.895
0.15	1.157	1.047	6.656	5.251	1.109	1.025	6.512	4.926	1.031	1.094	6.391	4.969
0.30	1.031	1.034	6.750	4.985	1.047	1.054	6.375	4.257	1.046	1.024	6.148	5.594
0.45	0.984	1.029	6.452	4.265	1.049	1.022	6.254	5.169	1.062	1.062	6.259	5.672
0.60	1.078	1.063	7.157	5.021	1.063	1.062	6.860	4.022	1.078	1.063	6.528	4.343
0.75	1.063	1.122	6.797	4.061	0.984	1.105	6.641	5.672	1.062	1.096	6.781	4.266
0.90	1.110	1.062	7.016	4.521	1.078	1.078	6.781	5.674.	.078	1.094	6.452	4.250